Chemistry–A European Journal | Research Article
doi.org/10.1002/chem.202200357
Chemistry Europe
European Chemical Societies Publishing

www.chemeurj.org

pH-Triggered Removal of Nitrogenous Organic Micropollutants from Water by Using Metal-Organic Polyhedra

Laura Hernández-López,[a, b] Alba Cortés-Martínez,[a, b] Teodor Parella,[c] Arnau Carné-Sánchez,*[a, b] and Daniel Maspoch*[a, b, d]

Abstract: Water pollution threatens human and environmental health worldwide. Thus, there is a pressing need for new approaches to water purification. Herein, we report a novel supramolecular strategy based on the use of a metal-organic polyhedron (MOP) as a capture agent to remove nitrogenous organic micropollutants from water, even at very low concentrations (ppm), based exclusively on coordination chemistry at the external surface of the MOP. Specifically, we exploit the exohedral coordination positions of Rh^{II}-MOP to coordinatively sequester pollutants bearing N-donor atoms in aqueous solution, and then harness their exposed surface carboxyl groups to control their aqueous solubility through acid/base reactions. We validated this approach for removal of benzotriazole, benzothiazole, isoquinoline, and 1-napthylamine from water.

Introduction

Hazardous organic micropollutants are found in natural water resources worldwide, posing a threat to human health and to ecosystems.[1,2] Thus, there is a pressing need to develop strategies and materials for water purification. Among the most efficient strategies for removal of organic micropollutants from water is adsorptive removal, which in some cases is followed by degradation of the pollutant. Effective adsorbents must combine high surface areas with strong chemical affinity for the target pollutants. Promising candidates include porous materials such as zeolites, activated carbon, covalent organic frameworks, and metal-organic frameworks, all of which offer large surface areas and whose pores can be chemically modified.[3–6] Other candidates are nanomaterials (e.g., nanoparticles, nanotubes, graphene, etc.), which boast high surface area-to-volume ratios, given their small size. Additionally, some nanomaterials exhibit highly reactive surfaces that can be functionalised for catalysing the degradation of the adsorbed pollutants.[7,8]

Researchers have recently begun to develop supramolecular strategies based on host-guest chemistry to capture and separate substances of interest.[9–12] In these strategies, discrete molecular compounds can be used in solution to selectively recognise, adsorb, and entrap the substance of interest inside their cavities.[13–16] The resultant host-guest complex is then isolated in solution by liquid/liquid extraction or phase transfer. Finally, the guest molecule is liberated from the host upon breakage of the host-guest interaction. For example, metal-organic coordination cages have been used to selectively separate specific polycyclic aromatic hydrocarbons from a mixture of similar molecules by phase-transfer phenomena.[17] Alternatively, multitopic ion-pair receptors based on calix[4]pyrrole derivatives have been employed to remove inorganics (K^+, Li^+, and Cs^+) from aqueous solution by liquid/liquid extraction.[18,19]

Our group recently reported an interesting alternative to the aforementioned host-guest approach to capture species of interest: rather than do coordination chemistry in the pores or cavities of molecular systems such as cages, we instead focus on coordination chemistry at the external surface of metal-organic cages or polyhedra (MOP). As proof-of-concept, we used the prototypical Rh^{II}-based MOP that comprises 12 divalent Rh–Rh paddlewheel clusters and 24 angular benzene-1,3-dicarboxylate (bdc) linkers, exhibits a cuboctahedral shape, and has an external diameter of 2.5 nm. Given the nanoscopic

[a] L. Hernández-López, A. Cortés-Martínez, Dr. A. Carné-Sánchez, Prof. D. Maspoch
Catalan Institute of Nanoscience and Nanotechnology (ICN2)
CSIC and The Barcelona Institute of Science and Technology
Campus UAB, Bellaterra, 08193 Barcelona (Spain)
E-mail: arnau.carne@icn2.cat
daniel.maspoch@icn2.cat

[b] L. Hernández-López, A. Cortés-Martínez, Dr. A. Carné-Sánchez, Prof. D. Maspoch
Departament de Química, Facultat de Ciències
Universitat Autònoma de Barcelona
08193 Bellaterra (Spain)

[c] Dr. T. Parella
Servei de Ressonància Magnètica Nuclear
Universitat Autònoma de Barcelona
Campus UAB, Bellaterra, 08193 Barcelona (Spain)

[d] Prof. D. Maspoch
ICREA
Pg. Lluís Companys 23, 08010 Barcelona (Spain)

Supporting information for this article is available on the WWW under https://doi.org/10.1002/chem.202200357

size and functional outer surface of this MOP, using it to capture species resembles the use of nanoparticle to do the same, albeit with the benefit of stoichiometric precision. This precision stems from the 84 available positions on the outer surface of the MOP, of two types. The first type, of which there are 12, are located in the 12 Rh–Rh paddlewheels. Each of these clusters expose a single exohedral axial coordination site that can be harnessed to bind coordinating molecules.

The second type, of which there are 72, derive from the 24 bdc linkers, each of which can be functionalised at three positions (4, 5 and 6) of its phenyl ring by conventional organic chemistry.[20] Our group previously demonstrated that this surface chemistry could be used to separate physicochemically similar molecules that differ in their affinity to the exohedral Rh^{II} axial site (separation by phase-transfer)[21] and in the steric hindrance around their coordinating atom (separation by liquid/liquid extraction).[22]

In the work that we report here, we adapted our previous surface chemistry approach to develop a new supramolecular strategy that uses the cuboctahedral Rh^{II}-MOP as a capture agent to remove organic micropollutants from water by pH-controlled precipitation (Figure 1). This strategy is based on combining the coordination ability of the Rh^{II} sites to capture organic pollutants that bear functional groups, with a simple acid-based reaction performed on the bdc linkers to control the solubility of the MOP in water. Thus, each one of the characteristic 12 exohedral axial coordination sites of these cuboctahedral Rh^{II}-MOPs is used to capture and bind coordinating pollutants from water by coordination chemistry. Moreover, among the different members of these cuboctahedral MOPs, we selected $[Rh_2(COOH\text{-}bdc)_2]_{12}$ (hereafter named COOHRhMOP; where COOH-bdc = 5-carboxy-1,3-benzenedicarboxylate). This MOP is functionalised with a carboxylic acid group at the 5-position of the phenyl ring of each bdc linker, such that its external surface is functionalised with a total of 24 carboxylic acid groups.[23] These groups are essential for our supramolecular strategy, as they confer the MOP with pH-dependent aqueous solubility. Indeed, when COOHRhMOP is exposed to a base (e.g., NaOH), it becomes an anionic, water-soluble MOP of formula $Na_{24}[Rh_2(COO\text{-}bdc)_2]_{12}$ (hereafter named COONaRhMOP; where COO-bdc = 1,3,5-benzenetricarboxylate). COONaRhMOP can then be reprotonated upon exposure to an acid (e.g., HCl), which precipitates it out from water such that it can be recovered by filtration or centrifugation. We envisioned that this pH-based solubility could serve as a trigger in a pollutant-removal system, reasoning that, once a coordinating molecule had become anchored to the surface of a MOP, the latter would govern the solubility of the former.

Thus, our supramolecular process for pollutant-removal is based on four steps. Firstly, coordinative interactions between the organic pollutant and the water-soluble COONaRhMOP are established in solution (Figure 1). Secondly, the COONaRhMOP-pollutant complex is precipitated out, by lowering the pH using HCl, and subsequently isolated from water by filtration or centrifugation. Thirdly, the precipitate is washed with aq. $CaCl_2$, leading to liberation of the pollutant. Through this washing step, Ca^{II} ions coordinate strongly to the organic micropollutant, breaking the COOHRhMOP-pollutant coordination interaction and dissolving the pollutant back into an aqueous solution. In the fourth and final step, the COOHRhMOP is treated with NaOH, causing it to redissolve in the remaining solution, which might contain residual pollutants, thereby enabling its reuse for subsequent cycles of water purification.

Results and Discussion

Removal of benzotriazole as a test-case. Step 1: Coordination between benzotriazole and COONaRhMOP in water

As proof-of-concept, we chose to test our MOP-based strategy by attempting to remove benzotriazole (BT) from water. Benzotriazole is broadly used both in industrial and household products: for instance, as a corrosion inhibitor; as an ultraviolet light-stabilizer in plastics; as an ultraviolet filter; as antifogging or defogging agent; and in de-icing/anti-icing fluids. The high amount of BT disposed by such activities, the high water-solubility of BT (ca. 20 $g \cdot L^{-1}$), and the slow biodegradation of BT lead to its high persistence in aquatic environments, where, at concentrations above about 5 ppm,[24,25] it causes environ-

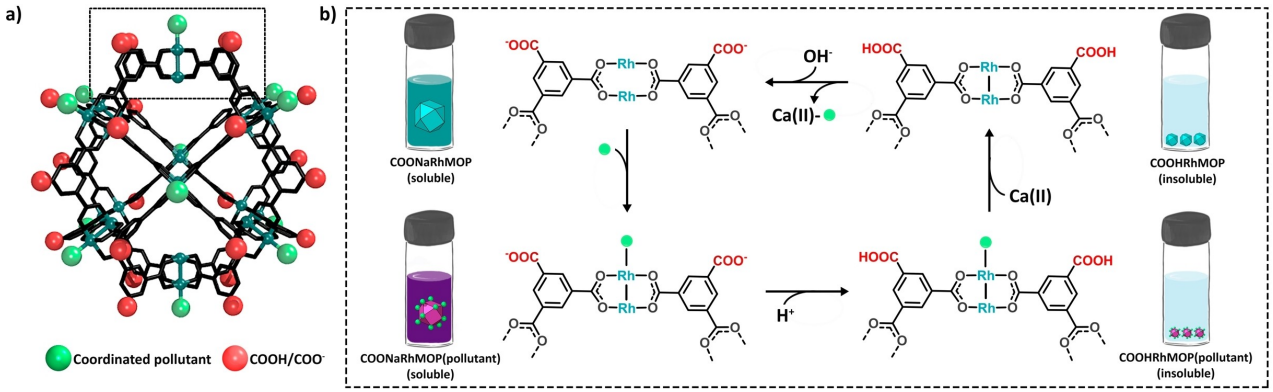

Figure 1. a) Structure of the cuboctahedral Rh^{II}-MOP, highlighting the 5-positions in the organic backbone (red balls) and the axial sites of its dirhodium paddlewheels (green balls). b) Schematic of the pH-triggered supramolecular removal strategy.

mental harmful long-term effects.[26–28] In fact, BT has been proposed as a micropollutant indicator of water contamination through anthropogenic activities, due to its ubiquity in surface water and its environmental toxicity.[29] Given that BT contains a triazole functional group fused to a benzene ring, we envisaged that we could anchor the molecule to the surface of COONaRhMOP, by coordinating the free N-donor atoms in the triazole of the former to the exposed axial sites of the Rh–Rh paddlewheels in the latter. To confirm this, we added BT to an aqueous solution of COONaRhMOP, and then monitored their interaction by naked eye. We found that the addition of BT (24 mol equiv, 380 ppm) to an aqueous solution of COONaRhMOP (0.133 μmol, 1 mL) induced an immediate change in colour of the solution, from blue to purple, suggesting a coordinative interaction between the BT and the Rh–Rh paddlewheel. Next, we monitored this interaction by UV-Vis spectroscopy, focusing on the bands centred at 500 to 600 nm, which correspond to the $\pi^* \rightarrow \sigma^*$ transitions (λ_{max}) of the Rh – Rh bonds. A shift in the Rh–Rh bond absorption band (λ_{max}), from 585 to 551 nm, corroborated coordination of the BT to the Rh–Rh paddlewheel (Figure S3 in the Supporting Information).[30,31] To further study the coordination of BT to the Rh–Rh paddlewheel units, we followed the titration of COONaRhMOP with BT by UV-Vis spectroscopy. We found that, below 10 mol equiv (159 ppm) of BT, the isosbestic point is preserved, indicating that each exohedral dirhodium axial site behaves independently.[22] Finally, we gained additional evidence that coordination of BT to COONaRhMOP proceeds through the exposed surface dirhodium axial sites, upon observing a marginal shift in λ_{max} above 12 mol equiv of BT (190 ppm).

Step 2: pH-triggered precipitation of COONaRhMOP(BT)

Having demonstrated the coordination of BT to COONaRhMOP, we reasoned that the captured BT could then be removed from water through in situ precipitation of the formed complex (hereafter named COONaRhMOP(BT)). Our hypothesis was based on the premise that, once the coordination between COONaRhMOP and BT had occurred, the solubility of the latter would be dictated by the solubility of the COONaRhMOP. Therefore, we expected that protonation of the surface carboxylate groups of COONaRhMOP(BT) would induce its precipitation, as we had already observed for COONaRhMOP alone (Figures S1 and S2). We expected that the precipitate (hereafter named COOHRhMOP(BT)) could then be easily removed by using simple techniques such as centrifugation or filtration. To this end, we optimised the pH at which a quantitative precipitation of the MOP occurs, while minimising protonation-induced cleavage of the BT–Rh^{II}–MOP coordination bond. These experiments were performed by preparing two different mixtures containing COONaRhMOP (0.133 μmol, 1 mL) and 6 mol equiv (95 ppm) or 24 mol equiv (380 ppm) of BT, being these two concentrations representative examples of defective and excess concentrations with respect to the 12 exohedral axial sites present in the MOP structure. Both resulting solutions (final pH = 8.6 and 7.8, respectively) were incubated for only 10 s and subsequently precipitated by lowering the pH with different amounts of HCl acid. The precipitation solids were isolated by centrifugation. Once the solids had been isolated, the optimum amount of acid for the precipitation process was determined by analysing the remaining BT in the aqueous solution after the precipitation step by means of UV-Vis measurements and establishing its removal efficiency (Figure S4). For both mixtures, the best performance was observed under milder acidic conditions when 10 μL of HCl 1 M (final pH = 2.3) were used to precipitate out the COOHRhMOP(BT). Based on this amount of acid, the following removal efficiency values were determined: 77% for the solution initially containing 6 mol equiv of BT; and 53% for the one containing 24 mol equiv of BT (see Section S3.5 in the Supporting Information). In both cases, the amount of MOP remaining in solution was lower than 0.1% (Table S1). Importantly, blank experiments (i.e., lacking COONaRhMOP) were performed in solution. These experiments revealed that the concentration of BT remained constant throughout the pH range studied (pH: 5.8 to 1.9), demonstrating the high aqueous solubility of BT and indicating that the solubility of the COOHRhMOP(BT) complex is indeed governed by that of COOHRhMOP itself (Figure S5).

Influence of the pH, the incubation time, and the concentration of BT on the removal efficiency

Once we had optimised the pH at which COOHRhMOP(BT) precipitates, we sought to elucidate the influence of the pH of the polluted water on the coordination of BT to COONaRhMOP and therefore, on the pollutant removal efficiency. This parameter might influence the removal efficiency of our proposed pH-triggered pollutant removal methodology due to the amphoteric properties of BT (pK_{a1}: 0.42, pK_{a2}: 8.27). To this end, we ran new experiments. Thus, three aqueous solutions containing COONaRhMOP (0.133 μmol, 1.03 mL) and BT (24 mol equiv; 380 ppm) were prepared. Each of these solutions, were brought to a different pH: either acidic (pH: 4.3), neutral (pH: 7.6) or basic (pH: 9.9). The UV-Vis spectrum of each aqueous phase revealed that the largest λ_{max} shifts were observed for the acidic conditions (Figure S10). This result is consistent with the fact that, at basic pH, BT can be deprotonated, which weakens its coordination to COONaRhMOP due to electrostatic repulsion. Contrariwise, acidic conditions lead to the formation of neutral BT, thereby favouring the formation of COONaRhMOP(BT) (Figure S9). However, these differences in the coordination of BT to COONaRHMOP did not translate into significative differences in the removal efficiencies after the precipitation step. Thus, after addition of the proper amount of diluted HCl (1 M) to each solution (1 μL to the acidic solution; 10 μL to the neutral one; and 10 μL to the basic one) to reach the optimised precipitating pH 2.3, the removal efficiency for BT was found to be around 54% in all cases (see Section S3.6). Altogether, these results highlight that our supramolecular strategy works in polluted water samples that vary in their initial pH level.

The experiments that we have described so far indicate that the interaction between COONaRhMOP and BT is fast, due to the absence of diffusion barriers, making a rapid method for pollutant removal feasible. To further confirm the lack of significant diffusion barriers in our proposed method, we performed new experiments to assess the impact of the incubation time prior the precipitation step on the BT removal efficiency. Accordingly, four independent aqueous solutions containing COOHNaRhMOP (0.133 μmol, 1 mL) and 6 mol equiv of BT (95 ppm) were prepared. Each solution was incubated for a different time (either 10 s, 10 min, 30 min, or 60 min), and then subjected to the aforementioned precipitation procedure. The UV-Vis spectra did not indicate any significant differences in the removal efficiencies, all of which were $>70\,\%$, suggesting that the incubation time does not influence the removal efficiency (Figure 2a, green dots, see Section S3.7.1). These results further confirmed the rapid capture and binding of BT to COONaRhMOP.

Once we had demonstrated that our pH-triggered, COONaRhMOP-based strategy could indeed remove BT from water, we next evaluated its performance at different concentrations of BT (Figure 2b, see Section S3.8). The initial and final concentrations were determined by either UV-Vis spectroscopy (conc. BT: >16 ppm) or ^{1}H NMR spectroscopy (conc. BT: <16 ppm; Figures S21 and S23). The consistency of the results obtained using both techniques was corroborated by analysing samples at an intermediate concentration (6 mol equiv, 95 ppm), using both techniques (Figures S21c and S22, Tables S6 and S7). The removal efficiency of BT for the solutions that had initially contained between 1 mol equiv (16 ppm) and 10 mol equiv (158 ppm) was found to be $>70\,\%$ in all cases, with a linear increase in BT removed per MOP with increasing initial conc. of BT (Figure 2b). Remarkably, the removal efficiency was up to 90 % in solutions that had contained BT at initial concentrations of 16 ppm. In this case, the remaining BT was below 1.6 ppm, which is below the level considered to be environmentally toxic (ca. 5 ppm).[24,25] Contrariwise, when 24 mol equiv (380 ppm) were initially present in the solution, the final amount of pollutant dropped to 10 mol equiv (158 ppm; removal efficiently: 55 %). These experiments confirmed that the ratio between pollutant and exohedral axial coordination metal sites in the COONaRhMOP determines the performance of our pH-triggered coordination-removal strategy.

Step 3: Regeneration and reusability of COOHRhMOP

Rapid and easy regeneration of the COOHRhMOP is essential for the feasibility of the proposed removal supramolecular strategy. Initially, we reasoned that exposing the COOHRhMOP(BT) solid to harsh acidic conditions would promote the formation of the protonated form of BT and consequently, its detachment from COOHRhMOP. However, we found that the detachment of BT required incubation under extremely acidic (3 M HCl) conditions, which we rule out, as they endangered the structural stability of the Rh^{II}-MOP (Figure S25). Alternatively, we sought a milder methodology that would entail washing of the precipitate with an aqueous solution containing a competing metallic centre for the coordination of BT. The formation of a new metal-BT complex would thus favour the regeneration of the occupied axial coordination sites of COOHRhMOP, whereby

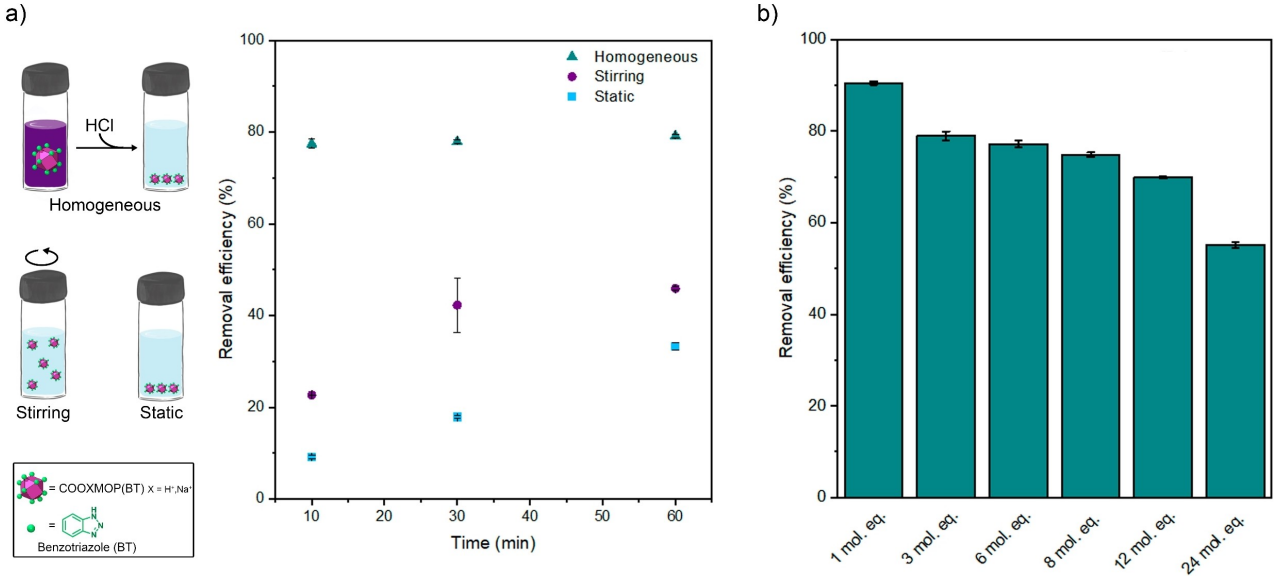

Figure 2. a) Left: Three methods for using COOHRhMOP to remove benzothiazole (BT; 6 mol equiv; 95 ppm) from water: as a porous solid under heterogeneous conditions, either with stirring or in a static reaction; or dissolved under homogeneous conditions, in our proposed, pH-triggered, supramolecular strategy. Right: Plot of the influence of reaction/incubation time on removal efficiency for each method: stirring, static, or homogeneous reactions. b) Removal efficiency of COONaRhMOP for BT at different concentrations of BT, ranging from 1 mol equiv (16 ppm) and 24 mol equiv (380 ppm), by using the supramolecular strategy. In both graphs, the data are reported as average values from triplicate experiments. Errors bars indicate standard deviation.

new uptake cycles could be performed. To this end, Ca^{II} was selected as a competing metallic centre, because of its reduced toxicity as well as its low cost. To explore its efficacy, we performed a preliminary washing experiment. To this end, the solid COOHRhMOP(BT) was washed twice by incubating it in a saturated solution of aq. $CaCl_2$ for 30 s. Note that this COOHRhMOP(BT) was initially precipitated from 5 mL solution of BT (6 mol equiv; 95 ppm), to which the removal strategy had earlier been applied using COONaRhMOP (0.67 μmol). After both washing steps, the remaining COOHRhMOP was quantitatively transformed into COONaRhMOP through basification with NaOH (16.1 μmol). This basification step caused the Rh^{II}-MOP to redissolve in the (now basic) aqueous solution. The success of the regeneration procedure was confirmed by UV-Vis analysis, as the initial λ_{max} of 583 nm characteristic of COONaRhMOP was obtained, thus further corroborating the detachment of BT from the outer surface of the Rh^{II}-MOP (Figures S26 and S27). Finally, the recovery and reusability of COONaRhMOP was confirmed by comparing the BT removal efficiency for three additional cycles of uptake (using the same conditions as in Cycle 1), precipitation, and regeneration. Remarkably, the recovered COONaRhMOP maintained its removal efficiency for BT for at least three consecutive cycles (Figures S28 and S29, Table S9). Moreover, the integrity of COONaRhMOP was maintained through the whole cycle, as evidenced by UV-Vis, ^{1}H NMR, and mass spectrometry (MS; see Section S3.10).

Use of filtration in the pH-triggered, supramolecular strategy

Next, we simplified our supramolecular strategy by replacing the centrifugation steps with a unified filtration process in which recovery of COOHRhMOP(BT), detachment of BT, and regeneration of COONaRhMOP occur sequentially. To this end, a test was run on 5 mL of a solution of BT (6 mol equiv; 95 ppm), to which the removal strategy was applied using COONaRhMOP (0.67 μmol). After precipitation with HCl, the aqueous solution was passed through a nylon syringe-filter (0.45 μm). The filter captured the COOHRhMOP(BT), observed as a purple solid, and the aqueous supernatant was recovered and analysed by means of UV-Vis spectroscopy (Figure 3a). This analysis revealed a comparable removal efficiency to that previously obtained (73%; Figures 3b, S33, Table S10). The filter was then treated with saturated aq. $CaCl_2$, which induced an immediate change in colour of the solid, from purple to blue, representative of cleavage of the Rh-BT coordination bond and subsequent release of the BT into the $CaCl_2$ solution. Finally, aq. NaOH was passed through the filter to redissolve the resultant COOHRhMOP, through formation of COONaRhMOP (Figures 3a and S34). Importantly, a blank experiment (i.e., without COOHRhMOP) revealed that the nylon syringe-filter alone does not contribute to any removal of BT (Figure S32). Interestingly, the strategy also proved successful when, instead of Milli-Q water, regular tap water was employed throughout the entire process (Section S3.12).

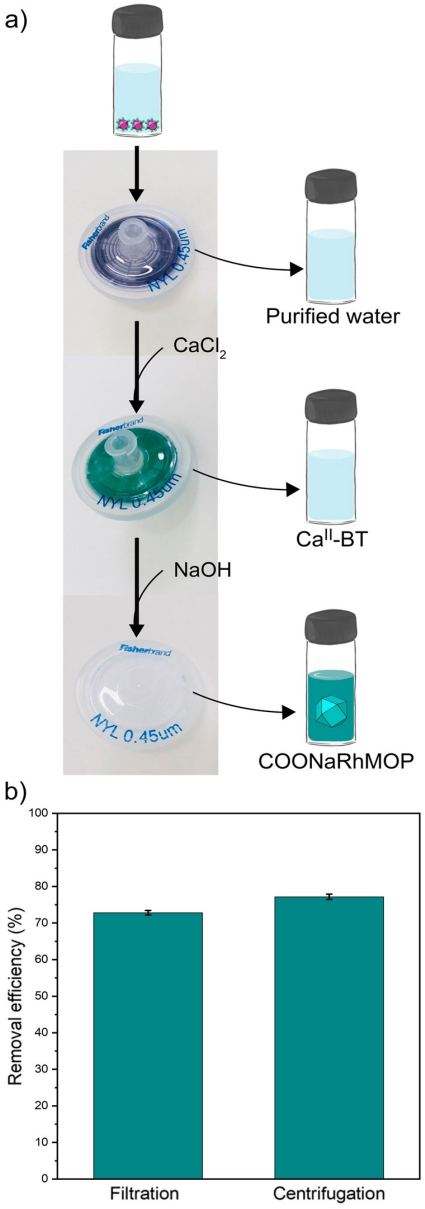

Figure 3. a) Schematic of the partial removal of BT by the pH-triggered, supramolecular strategy using filtration (rather than centrifugation) to isolate the capture agent. b) Comparison of removal efficiency for filtration vs. centrifugation. The data are reported as the average uptake value from duplicate experiments. Error bars indicate the standard deviation.

Comparison of the removal of benzotriazole using COOHRhMOP as a porous solid

To evaluate the possible influence of classical diffusion barriers on the efficiency of COOHRhMOP at removing BT from water, we next ran tests under heterogeneous conditions. To this end, COOHRhMOP powder (5 mg, 0.67 mmol) was soaked in a solution containing BT (6 mol equiv; 95 ppm; 5 mL) at a pH of 6.0. This pH was selected to ensure that the MOP remains in its neutral form, and that the BT is predominantly in its more-coordinative state. The heterogeneous removal tests were performed both with stirring and without (hereafter called

static), and the removal efficiency was quantified after different incubation times. Interestingly, the removal efficiency was slightly higher in the stirred reactions (46%) than in the static one (33%; Figure 2b, purple and sky-blue dots, and Section S3.7.2). For both conditions, the best performance was observed after 1 h of incubation. Altogether, these results evidence the detrimental effect of diffusion barriers in the coordination of BT to COOHRhMOP under when used as a solid powder (i.e., heterogeneous conditions), for which the kinetics are less favourable – and consequently, the removal efficiency, lower – compared to using COONaRhMOP in solution (i.e., homogeneous conditions).

Expanding the scope of the pH-triggered coordinative-removal supramolecular strategy

We reasoned that our strategy might become more challenging to apply to removal of pollutants that contain coordinating groups that are more pH-sensitive than BT, as protonation of these groups preclude the interaction between the pollutant and the COONaRhMOP. To explore this hypothesis, we tested the performance of our strategy at removing other nitrogenous organic micropollutants from water, whose coordinating groups are easier to protonate than are the coordinating N-atoms in the triazole ring of BT (pK_{a1}: 0.42). Thus, we chose three polar pollutants commonly found in water: i) benzothiazole (BTZ; pK_a: 2.28), which is used as vulcanisation accelerator in rubber manufacture and as an herbicide;[32,33] ii) 1-naphtylamine (NA; pK_a: 4.25), used both as a fungicide and as a precursor of azo-dyes, which is classified as a carcinogen;[34,35] and iii) isoquinoline (IQ; pK_a: 5.26),[36,37] which is a potentially genotoxic compound found in coking wastewaters (Figure 4, right). Firstly, the coordination of BTZ, NA, or IQ to COONaRhMOP was confirmed by UV-Vis spectroscopy (Figures S37, S50 and S66). Then, the precipitation conditions for each pollutant were optimised, using a similar approach to that previously followed for BT,

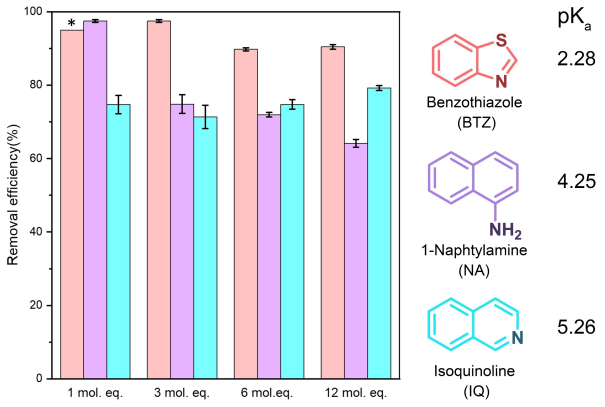

Figure 4. Efficiency of COONaRhMOP at removing BTZ, NA, and IQ from aqueous solutions. *A removal efficiency of > 95% was assumed for BTZ at 1 mol equiv (18 ppm) because the residual concentration of BTZ in the remaining aqueous solution was below the limit of quantification (0.9 ppm). All values are reported as an average of triplicate experiments. Errors bars indicate standard deviation.

whereby a balance between the removal efficiency and the complete precipitation of COOHRHMOP(pollutant) was found. For all these experiments, UV-Vis and ^{1}H NMR were employed to quantitatively evaluate the removal efficiency. As depicted in Figure 4, very high removal efficiencies were found for BTZ (ca. 80% to 90%) throughout the tested concentration range, with values even higher than those for BT. We attributed this performance to the greater hydrophobicity of BTZ relative to BT, which facilitates its removal from water (Section S4.2.4). The removal of pollutants containing weak bases/nucleophiles could be limited by the weakness of the coordination bonds. However, despite the weak coordination observed between NA and the dirhodium paddlewheel (Figure S50), the removal efficiency for NA was 80% at low concentrations (1 mol equiv; 19 ppm; Section S4.3.4). Moreover, although the required pH for the precipitation of either COOHRhMOP(NA) or COOHRhMOP(IQ) was lower (ca. 3.5) than the reported pK_a for either NA or IQ, the removal efficiency for both pollutants was 70% (Sections S4.3.4 and S4.4.4). These results confirm that the respective coordinative bonds remain intact at these (more acidic) pH values. Lastly, in all cases, the complexes obtained from precipitation were recoverable again by using Ca^{II} as a competing metallic centre for the coordination of the organic coordinating pollutants). Note that both NA and IQ could also be recovered by using an acidic (0.3 M HCl) wash, as their easier protonation allowed the complete recovery without endangering the MOP structure. Additionally, the recovered materials were reusable, as they demonstrated comparable removal efficiency values in subsequent cycles structure (Sections S4.2.5, S4.3.5 and S4.4.5). The integrity of COONaRhMOP was further evidenced by UV-Vis, ^{1}H NMR, and MS (Sections S4.2.6, S4.3.6 and S4.4.6).

Simultaneous removal of multiple nitrogenous organic micropollutants from an aqueous solution

Encouraged by our results, we envisaged that we could use our pH-triggered supramolecular strategy to simultaneously remove multiple organic pollutants from water. To this end, we performed a test in an aqueous solution containing a mixture of BT, BTZ, NA, and IQ. Thus, a 3 mL of an aqueous solution containing COONaRhMOP (0.4 μmol) and equimolar mixture of BT (6 mol equiv; 95 ppm), BTZ (6 mol equiv; 108 ppm), NA (6 mol equiv; 114 ppm), and IQ (6 mol equiv; 102 ppm) was prepared. Then, this mixture was subjected to multiple cycles of pollutant removal/capture-agent regeneration. As indicated by ^{1}H NMR spectra taken before and after the first cycle, the removal efficiency values were, from highest to lowers: 87% (BTZ), 85% (NA), 74% (IQ) and 66% (BT; Figure 5). Although a similar value was observed for removal of BTZ from this multi-pollutant solution compared to from the mono-pollutant solution, the corresponding values for the other pollutants did differ. Interestingly, the values for removal of NA and IQ were higher than from the respective mono-pollutant solutions, whereas that for BT was slightly lower. Overall, these values confirm that each COONaRhMOP can capture more than 12

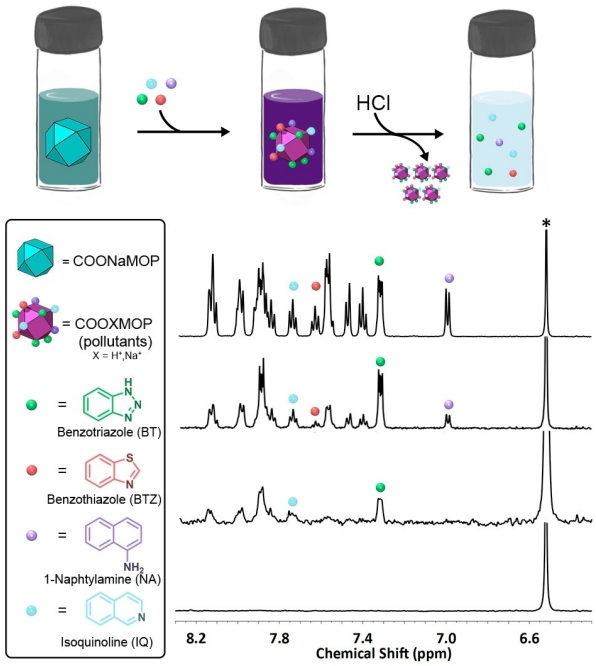

Figure 5. Top: Schematic of the simultaneous removal of various organic micropollutant pollutants from an aqueous multipollutant solution by the pH-triggered, supramolecular strategy. Bottom: Stacked ^{1}H NMR spectra of a D_2O solution before (top) and after three subsequent (from high to low) removal/regeneration cycles. Left: Legend for both parts.

pollutant molecules (ca. 20). We attributed the results to the contribution of cooperative hydrophobic and Van der Waals interactions, which can enhance the performance of the capturing agent once all the specific binding sites have been occupied. Next, the capture agent was regenerated, and the remaining aqueous solution with the four residual pollutants was subjected to additional removal/regeneration cycles. By the second cycle, all of the BTZ and NA had been fully removed, and by the third cycle all of the BT and IQ had been removed (Section S5.3). Again, the stability of the COONaRhMOP was maintained throughout each cycle, as confirmed by UV-Vis, ^{1}H NMR, and MS (Section S5.4).

Conclusion

Through this proof-of-concept study, we have demonstrated that robust, water-soluble MOPs can be harnessed to remove organic pollutants from water in a pH-triggered fashion. We engineered a novel organic-pollutant removal supramolecular strategy based on the pH-dependent solubility of COOHRhMOP. At high pH, the anionic, water-soluble COONaRhMOP is formed, whose outer surface interacts, through coordination chemistry, with organic pollutants bearing basic N-donor atoms. A rapid decrease in pH forces the precipitation of the resultant MOP-pollutant complex from purified water. We demonstrated the efficacy of our approach at removing four common micro-pollutants – benzotriazole, benzothiazole, isoquinoline, and 1-napthylamine – from water at various concentrations, using both single and multiple-pollutant solutions. In all cases, the COOHRhMOP can be easily regenerated by using readily available and mild reagents ($CaCl_2$ and NaOH), and its performance is maintained through multiple cycles of removal/regeneration. Our work lays the foundation for the development of pH-induced precipitation of organic pollutants, akin to currently used methods for the removal of inorganic salts. Moreover, we envisage that the wide structural versatility of MOPs will enable our approach to be extended to many other organic pollutants, especially by exploiting other MOP-pollutant interactions than (or in addition to) coordination chemistry, including host-guest, π–π and electrostatic interactions, and combinations thereof. Thus, the results presented here widen the scope of applications for the emerging water-soluble metal-organic cages toward pollutant removal and environmental applications.[38]

Acknowledgements

This work was supported by the Spanish MINECO (project RTI2018-095622-B–I00) and the Catalan AGAUR (project 2017 SGR 238). It was also funded by the CERCA Programme/ Generalitat de Catalunya and through a fellowship (LCF/BQ/PR20/11770011) from the "la Caixa" Foundation (ID 100010434). ICN2 is supported by the Severo Ochoa programme from the Spanish MINECO (grant no. SEV-2017-0706). L.H.L. acknowledges the support from the Spanish State Research Agency (PRE2019-088056).

Conflict of Interest

The authors declare no conflict of interest.

Data Availability Statement

The data that support the findings of this study are available on request from the corresponding author. The data are not publicly available due to privacy or ethical restrictions.

Keywords: coordinative removal · metal-organic polyhedra · pH-responsive · organic micropollutants · pollutant removal

[1] R. P. Schwarzenbach, B. I. Escher, K. Fenner, T. B. Hofstetter, C. A. Johnson, U. von Gunten, B. Wehrli, *Science* **2006**, *313*, 1072–1077.
[2] S. D. Richardson, T. A. Ternes, *Anal. Chem.* **2014**, *86*, 2813–2848.
[3] M. Mon, R. Bruno, J. Ferrando-Soria, D. Armentano, E. Pardo, *J. Mater. Chem. A* **2018**, *6*, 4912–4947.
[4] M. Mon, R. Bruno, E. Tiburcio, M. Viciano-Chumillas, L. H. G. Kalinke, J. Ferrando-Soria, D. Armentano, E. Pardo, *J. Am. Chem. Soc.* **2019**, *141*, 13601–13609.
[5] J. L. Fenton, D. W. Burke, D. Qian, M. Olvera de la Cruz, W. R. Dichtel, *J. Am. Chem. Soc.* **2021**, *143*, 1466–1473.
[6] S. Rojas, P. Horcajada, *Chem. Rev.* **2020**, *120*, 8378–8415.
[7] J. You, L. Wang, Y. Zhao, W. Bao, *J. Cleaner Prod.* **2021**, *281*, 124668.
[8] L. Marcon, J. Oliveras, V. F. Puntes, *Sci. Total Environ.* **2021**, *791*, 148324.

[9] B. Shi, H. Guan, L. Shangguan, H. Wang, D. Xia, X. Kong, F. Huang, *J. Mater. Chem. A* **2017**, *5*, 24217–24222.
[10] L.-P. Yang, H. Ke, H. Yao, W. Jiang, *Angew. Chem. Int. Ed.* **2021**, *60*, 21404–21411.
[11] X. Wang, L. Xie, K. Lin, W. Ma, T. Zhao, X. Ji, M. Alyami, N. M. Khashab, H. Wang, J. L. Sessler, *Angew. Chem. Int. Ed.* **2021**, *60*, 7188–7196.
[12] D. Zhang, T. K. Ronson, Y. Q. Zou, J. R. Nitschke, *Nat. Chem. Rev.* **2021**, *5*, 168–182.
[13] D. Zhang, T. K. Ronson, J. Mosquera, A. Martinez, J. R. Nitschke, *Angew. Chem. Int. Ed.* **2018**, *57*, 3717–3721; *Angew. Chem.* **2018**, *130*, 3779–3783.
[14] Y. J. Hou, K. Wu, Z. W. Wei, K. Li, Y. L. Lu, C. Y. Zhu, J. S. Wang, M. Pan, J. J. Jiang, G. Q. Li, C. Y. Su, *J. Am. Chem. Soc.* **2018**, *140*, 18183–18191.
[15] H. N. Zhang, Y. Lu, W. X. Gao, Y. J. Lin, G. X. Jin, *Chem. Eur. J.* **2018**, *24*, 18913–18921.
[16] A. B. Grommet, J. B. Hoffman, E. G. Percástegui, J. Mosquera, D. J. Howe, J. L. Bolliger, J. R. Nitschke, *J. Am. Chem. Soc.* **2018**, *140*, 14770–14776.
[17] D. Zhang, T. K. Ronson, R. Lavendomme, J. R. Nitschke, *J. Am. Chem. Soc.* **2019**, *141*, 18949–18953.
[18] Q. He, N. J. Williams, J. H. Oh, V. M. Lynch, S. K. Kim, B. A. Moyer, J. L. Sessler, *Angew. Chem. Int. Ed.* **2018**, *57*, 11924–11928.
[19] S. K. Kim, B. P. Hay, J. S. Kim, B. A. Moyer, J. L. Sessler, *Chem. Commun.* **2013**, *49*, 2112–2114.
[20] A. Carné-Sánchez, J. Albalad, T. Grancha, I. Imaz, J. Juanhuix, P. Larpent, S. Furukawa, D. Maspoch, *J. Am. Chem. Soc.* **2019**, *141*, 4094–4102.
[21] T. Grancha, A. Carné-Sánchez, L. Hernández-López, J. Albalad, I. Imaz, J. Juanhuix, D. Maspoch, *J. Am. Chem. Soc.* **2019**, *141*, 18349–18355.
[22] L. Hernández-López, J. Martínez-Esaín, A. Carné-Sánchez, T. Grancha, J. Faraudo, D. Maspoch, *Angew. Chem. Int. Ed.* **2021**, *60*, 11406–11413.
[23] J. Albalad, A. Carné-Sánchez, T. Grancha, L. Hernández-López, D. Maspoch, *Chem. Commun.* **2019**, *55*, 12785–12788.
[24] A. Seeland, M. Oetken, A. Kiss, E. Fries, J. Oehlmann, *Environ. Sci. Pollut. Res. Int.* **2012**, *19*, 1781–1790.
[25] Y.-J. Shin, B. Kim, H. Kim, K. Kim, K. Park, J. Kim, H. Kim, P. Kim, *Sci. Total Environ.* **2022**, *815*, 152846.
[26] M. D. Alotaibi, A. J. McKinley, B. M. Patterson, A. Y. Reeder, *Water Air Soil Pollut.* **2015**, *226*, 226.
[27] T. V. Wagner, J. R. Parsons, H. H. M. Rijnaarts, P. de Voogt, A. A. M. Langenhoff, *J. Hazard. Mater.* **2020**, *384*, 121314.
[28] T. Reemtsma, U. Miehe, U. Duennbier, M. Jekel, *Water Res.* **2010**, *44*, 596–604.
[29] M. Jekel, W. Dott, A. Bergmann, U. Dünnbier, R. Gnirß, B. Haist-Gulde, G. Hamscher, M. Letzel, T. Licha, S. Lyko, U. Miehe, F. Sacher, M. Scheurer, C. K. Schmidt, T. Reemtsma, A. S. Ruhl, *Chemosphere* **2015**, *125*, 155–167.
[30] E. B. Boyar, S. D. Robinson, *Coord. Chem. Rev.* **1983**, *50*, 109–208.
[31] E. Warzecha, T. C. Berto, C. C. Wilkinson, J. F. Berry, *J. Chem. Educ.* **2019**, *96*, 571–576.
[32] L. Wang, J. Zhang, H. Sun, Q. Zhou, *Environ. Sci. Technol.* **2016**, *50*, 2709–2717.
[33] C. Liao, U.-J. Kim, K. Kannan, *Environ. Sci. Technol.* **2018**, *52*, 5007–5026.
[34] J. Hu, D. Shao, C. Chen, G. Sheng, X. Ren, X. Wang, *J. Hazard. Mater.* **2011**, *185*, 463–471.
[35] W. Zhang, C. Hong, B. Pan, Z. Xu, Q. Zhang, L. Lv, *J. Hazard. Mater.* **2008**, *158*, 293–299.
[36] D. R. Joshi, Y. Zhang, H. Zhang, Y. Gao, M. Yang, *J. Environ. Sci.* **2018**, *63*, 105–115.
[37] K. V. Padoley, S. N. Mudliar, R. A. Pandey, *Bioresour. Technol.* **2008**, *99*, 4029–4043.
[38] E. G. Percástegui, T. K. Ronson, J. R. Nitschke, *Chem. Rev.* **2020**, *120*, 13480–13544.

Manuscript received: February 4, 2022
Accepted manuscript online: March 29, 2022
Version of record online: April 22, 2022